Electron density and temperature profiles from spectroscopy in the upper divertor plasma of ASDEX Upgrade

R. Dux, H. Lindl, and the ASDEX Upgrade team

Max-Planck-Institut für Plasmaphysik, Garching, Germany.

The analysis of advanced divertor configurations in the new upper divertor of ASDEX Upgrade requires measurements of electron density and temperature profiles not only at the target but also in the volume of the divertor plasma. In addition to a new Thomson scattering diagnostic in the upper divertor, a new spectroscopic diagnostic has been setup to deliver this information.

Optical setup

The almost horizontal upper divertor target plate allows for a much better observation of the divertor plasma compared to the rather closed divertor geometry of the lower divertor with vertical strike point tiles. Four optical heads were installed which observe the divertor plasma with purely toroidal viewing geometry, i.e. each head has lines-of-sight (LOS) at a constant height Z and probes the plasma with different tangency radii. The heads are at a height of about 43, 74, 114, and 172 mm below the centre of the target plate. Two heads have quartz lenses with a focal length f=60 mm (f#=3.5) and are equipped with 10 fibres, while the other two have f=103 mm (f#=3.8) and 15 fibres. The tangency radii have an average distance of $\sim$16 mm for the 103 mm-heads and $\sim$ 21 mm for the 60 mm-heads and the corresponding diameter of the fibre image is 5.6 mm and 8.3 mm. In order to minimise reflections, the LOS end on boron coated graphite tiles, which have a black surface. The bidirectional reflectance of the boron surface has been measured for several wavelengths and angles and was found to be constant without a peak around the angle for specular reflection. Thus, it can be well described by a perfectly diffuse "Lambertian" reflecting surface with a reflectance of f_r= 2.3×10^{-2} sr^{-1}, such that 7.2% of the incoming radiation is isotropically reflected into the whole hemisphere. This value is so low, that model calculations with and without reflections show no influence of the reflected light on the evaluated radiation distribution inside the plasma. The quartz fibres from each head are guided out of the torus to a switchboard in the spectroscopy lab, where they can be connected to various grating spectrometers. Each spectrometer has a grating with 2400 lines per mm and the focal length varies between 180 mm for the most sensitive devices with f#=2.8 and 1000 mm for the high resolution systems with f#=10. Each spectrometer measures the spectra of all fibres of one head using a CCD-camera with a minimal temporal resolution of 2 ms. The whole optical setup, from the heads up to the CCD-cameras, has been absolutely calibrated by placing an integrating sphere in front of the heads such that the spectral radiance can be gained from the measured count rate. The wavelength setting of the spectrometer is calibrated at each discharge by measuring neon or mercury lines of spectral calibration lamps.

Abel transformation of the spectral radiances using a forward model

A forward model has been set up to calculate the spectral radiances from the radial profiles of line emissivities, temperatures, parallel velocities, and electron densities. A non-linear fit op-

timises the parameters which describe these profiles until the best agreement with the measured spectra of the radiances on all n LOS of one head is obtained. In the model, the spectral radiance $L_{k,\lambda}$ on LOS k is given by

$$L_{k,\lambda} = \int_{R_k}^{R_{\max}} \left(\varepsilon_{b,\lambda} + \sum_{m=1}^{M} \varepsilon_L^m S_\lambda^m(n_e, T, v_\parallel, B, \theta_k) \right) \frac{2R}{\sqrt{R^2 - R_k^2}} dR \tag{1}$$

All parameters inside the large brackets depend on R and R_k is the tangency radius of LOS k. The integration goes from the tangency radius of the LOS up to R_{max}, which is not known and has to be estimated. The total spectral radiance is the sum of a continuum value $\varepsilon_{b,\lambda}$, which is taken to be constant within the considered wavelength range, and M multiplets emitted from impurities or hydrogen. Each multiplet is described by the product of a line emissivity ε_L^m and a line shape function $S_\lambda^m(n_e, T, v_\parallel, B, \theta_k)$. The line shape function is normalised to one

$$\int_0^\infty S_\lambda^m d\lambda = 1 \tag{2}$$

and contains the influence of the Doppler broadening via $T(R)$, the Doppler shift via $v_\parallel(R)$, the line splitting due to the magnetic field $B(R)$, the angle θ_k between B-field and LOS, the electron density $n_e(R)$ due to the Stark effect for the hydrogen lines, and the instrumental line shape of the used spectrometer. The magnetic field strength is strongly dominated by the toroidal field and the cosine of the angle θ_k simply is $\cos\theta_k = R_k/R$. The radial profiles of all parameters are described by cubic splines function $f_c(R)$ with natural boundary conditions, i.e. zero second derivatives at the inner boundary R_n and at the outer boundary R_1. The profile is set to be constant between R_1 and R_{max}. The values at the n knots are the free fit parameters for each profile. Almost all profiles besides the parallel velocity must be positive, hence for these quantities the exponential of the spline function is used in the forward model. For spectrometers with lower resolution, some of the spectral line broadening mechanisms are negligible compared to the instrumental line shape and the respective parameters can be set to a fixed value, thus reducing the number of free parameters in the non-linear fitting routine. The spectra are first fitted by a χ^2-fit of the parameters. Then, a measure for the curvature of the spline functions: $C = \int f_c''(R)^2 dR$ of the most important parameters is evaluated and when above a preset goal of the curvature, the fit is repeated, but now minimising the weighted sum of χ^2 and the sum of the curvature integrals. The preset curvature goal is related to the expected strength of oscillations in the observed divertor plasma.

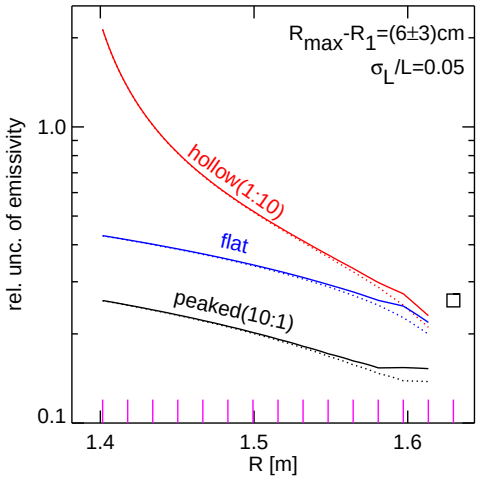

Fig.1: *Relative uncertainty of the emissivity profiles obtained from the Abel transformation of the uncertain radiances for three model cases with peaked, flat, and hollow emissivity profiles.*

The uncertainty of the fitted line emissivity profiles depends on the shape of the emissivity profile and has been evaluated for three model cases (see Fig.1). We assume for the measured radiances L a relative uncertainty of σ_L/L=5% for all 15 LOS (tangency radii of the LOS are shown with magenta lines at the bottom of Fig.1). A linear emissivity function was used, which was either decreasing by a factor of 10 between the tangency radii of the innermost and outermost LOS (peaked), constant (flat), or increasing by a factor of 10 (hollow). The Abel transformation leads to weighted differences of the radiances at the inner LOS minus the radiances at the outer LOS. For the peaked profile, the radiances at the outer LOS are low and the relative uncertainty increases up to 26% for the innermost radius. For the hollow case, the transform is much more uncertain with $\sigma_\varepsilon/\varepsilon$=2 at the innermost radius. The σ_L-contribution to σ_ε is shown with the dashed lines in Fig.1. The boundary R_{max} was set to be 6 cm larger than the outermost tangency radius R_1 with an uncertainty of 50% for $R_{max}-R_1$. For all profiles, this produces an uncertainty of about 25% for the emissivity at R_1 since the radiance increases with $\sqrt{R_{max}-R_1}$ (square symbol in Fig.1). For smaller radii, the total uncertainty including $\sigma(R_{max})$ is depicted with solid lines and shows that the influence of $\sigma(R_{max})$ decreases with radius. For further analysis we just use the profiles up to R_2.

Electron Density and Temperature from high-n Balmer lines

The spectra of a high-n Balmer line, i.e. D_ε (n=7-2), allow to access the radial electron density profiles $n_e(R)$ via the Stark broadening, which is rather strong with a detection threshold of about $n_e \approx 4\times10^{19}\,\mathrm{m}^{-3}$. Furthermore, the line emissivity profile $\varepsilon_L(R)$ of D_ε, i.e. the number of photons emitted per volume, time, and steradian is a very valuable result of the fit procedure. From ε_L and n_e, the radial profiles of the electron temperature $T_e(R)$ can be obtained. This is possible since the three body recombination, i.e. the inverse process of the electron impact ionisation, is much more frequent than the radiative recombination and the ionisation time scale is much shorter than transport time scales, such that the Saha equilibrium between the bound electrons in the high-n state and the free electrons is established at the local electron temperature. The collisional-radiative model of D was analysed using the method described in [1]. It yields that at n_e=$1\times10^{20}\,\mathrm{m}^{-3}$, ε_L deviates from the Saha equilibrium value by less than 1% for T_e=0.5-50 eV (see Fig.2) while the equilibration is established on time scales shorter than 5 ns.

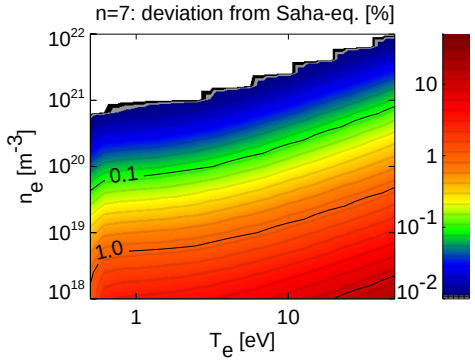

Fig.2: *n_e, T_e map showing the deviations of the population in the n=7-level from Saha-equilibrium values in percent.*

First measurement with Alternative Divertor Configuration (ADC)

For divertor plasmas in the parameter range of interest, i.e. cold plasmas near detachment, the measured radiances are very strong, as they scale with $\varepsilon_L \propto n_e^2 T_e^{-3/2}$. Fig.3 gives an impression

of the obtainable profiles. The data are for discharge #42949 at t=3.9 s, an H-mode plasma with I_p=800 kA, B_T=2.6 T, 6.5 MW of external heating, and nitrogen puffing. The flux surfaces shown in Fig.3 are separated by 2 mm steps when measuring their distance ΔR_{om} to the separatrix at the outboard midplane. The primary X-point is at (R,Z)=(1.51,1.04) m and a secondary X-point is at (1.39,1.04) m with ΔR_{om} of just 0.7 mm. The color bars give ε_L of D$_\varepsilon$, n_e from Stark broadening, T_e from the Saha-equilibrium of D in n=7, and ε_L of the transition $2s^2 2p3p\ ^1D \rightarrow 2s^2 2p3s\ ^1P$ of N^+ at 399.5 nm. The lowest T_e values of slightly below 0.5 eV are in the private flux region above the primary X-point. They increase to around 14 eV in the near SOL at Z=0.98 m and around 11 eV at Z=0.93 m in the confined region. In the private flux region n_e is around 2×10^{20} m^{-3} , around 5×10^{20} m^{-3} in the hotter SOL, and around 9×10^{20} m^{-3} in the confined plasma. The N^+-line has very low emission when T_e is below 1 eV (private flux region). Around the primary X-point, the N^+ emission is still about a factor 40 lower than the maximum value further down at Z=0.93 m in the confined region where n_e and T_e is higher.

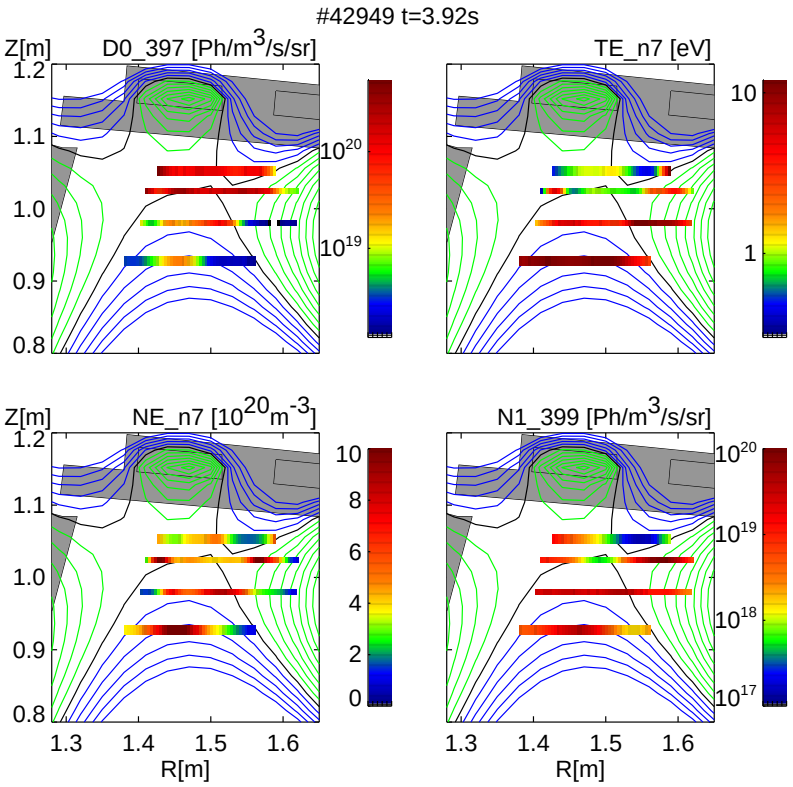

Fig.3: *Radial profiless of the line emissivty of D_ε, T_e, n_e, and the line emissivty of a N^+-line at 399.5 nm for the four heads measured in #42949 at t=3.9 s.*

It can be concluded, that the first data look rather promising and that this new spectroscopy approach is a useful method to quantify the processes in the volume of the divertor plasma.

Acknowledgement

This work has been carried out within the framework of the EUROfusion Consortium, funded by the European Union via the Euratom Research and Training Programme (Grant Agreement No 101052200 — EUROfusion). Views and opinions expressed are however those of the author(s) only and do not necessarily reflect those of the European Union or the European Commission. Neither the European Union nor the European Commission can be held responsible for them.

References

[1] D.R. Bates, A.E. Kingston, R.W.P. McWhirter, Proc. Royal Soc. of London Series A, **267** (1962) 297.